Finite element analysis of coupled electronic states in quantum dot nanostructures

R V N Melnik[1,3] **and K N Zotsenko**[2]

[1] University of Southern Denmark, Mads Clausen Institute for Product Innovation, Sonderborg, DK-6400, Denmark
[2] Electronic Data Systems Australia, 60 Currington Street, Sydney, NSW 2000, Australia

E-mail: melnik_rvn@member.ams.org

Abstract
Nanostructures, created by confinement of the motion of an electron from all three dimensions and known as quantum dots (QDs), provide materials scientists with a wide range of potential applications. These structures are produced today with advances of QD growth technology, and computational tools are fundamental in providing a better understanding of such structures. In this paper QD nanostructures are analysed with due account for coupling effects between electronic states in the dot and the wetting layer regions. The analysis, performed on the basis of the finite element methodology and Arnoldi iterations, demonstrates that the effect of coupling may be essential. The numerical procedure applied here is more efficient compared to the QR algorithm typically used in the context of modelling low-dimensional nanostructures. We report results of computational experiments for cylindrical and truncated conical QDs and compare them with the earlier results obtained for fully conical QD nanostructures.

1. Introduction

The development of nanotechnological and microelectronics applications has provided some of the most challenging problems in computational science [1]. Moving to nanosize devices opens new opportunities for computational scientists, and many important problems in nanoscience have already been solved with computational tools.

Semiconductor structures can be fabricated with practically unlimited flexibility, and the formation of self-assembled quantum dots (QDs) have been demonstrated in several different materials. These low-dimensional structures, where the electron motion is confined from all

---

[3] Author to whom any correspondence should be addressed.

three dimensions, are expected to play a pivotal role in many micro- and nano-optoelectronic applications.

The major focus of this paper is on modelling such semiconductor nanostructures, emphasizing the effects of coupling between electronic states in the QD and the wetting layer (WL) regions. One of the primary reasons for that lies with the fact that at present there exist several methodologies such as the Stranski–Krastanow technique that allow us to produce electronic states confined from all three dimensions. The Stranski–Krastanow methodology is essentially a self-organized hetero-epitaxial growth during molecular beam epitaxy technique. When this methodology is applied, the resulting 'QD' structures consist of two distinctively different regions, the QD region and the WL region. The size and shape of such 'quantum islands' depend substantially on the growth conditions and the technique used. The properties of the structure resulting from this growth process are dependent on thermal, elastic, piezoelectric, and other effects, and controlling the process is a difficult task [2] which can be assisted by computational experiments. The structures themselves can be grown in different shapes such as conical, truncated conical, pyramidal, and cylindrical. The geometry of the structure influences substantially such important characteristics as optoelectronic properties of the quantum device, as do different effective masses in the dot and the crystal matrix of such devices [3,4]. Cylindrical-shaped QDs, conical and truncated conical and pyramidal QDs have been analysed computationally earlier (e.g. [5–7] and references therein) and considerable efforts have been directed towards the experimental analysis of these structures [8]. However, most studies of electronic bandstructures still exclude the WL from consideration, and no prior systematic investigation of the influence of the WL on electronic states of the entire structure have been carried out. A better understanding of this influence is important in evaluating optical properties of low-dimensional nanostructures (e.g. [9]), and we aim at using a relatively simple mathematical model to demonstrate that this influence may be essential. Recently, it was shown that the inclusion of the WL, a 'substrate' on which the dot is grown, leads to a situation where the WL electronic states and the states of the QD are essentially coupled [10]. Only a specific type of conical geometry was considered. It is our purpose in this paper to extend those results and further examine this coupling for cylindrical and truncated conical QDs.

2. Position-dependent effective mass model for coupled QD–WL nanostructures

In this paper, we consider InAs QDs embedded in GaAs matrices. We start our consideration from the full three-dimensional model of the QD by using the envelope function approximation. The discussion is focused on the one-band model as an example, in which case the Hamiltonian of the system can be represented in the following form (e.g. [11]):

$$H = -\frac{\hbar^2}{2}\nabla_r \cdot \left(\frac{1}{m(r)}\nabla_r\right) + V(r), \tag{2.1}$$

where $m(r)$ is the position-dependent electron effective mass, $\hbar$ is Planck's constant divided by 2π, and $V(r)$ is the confinement (band-edge) potential. Although it is often assumed that the electron effective mass is a constant inside of the domain of interest, this assumption cannot be justified for any real considerations since $m(r)$ is a function of position and varies considerably between two major regions of interest, InAs and GaAs in this paper. Taking this difference into account is essential, but this is connected with the necessity to interpret the model

$$H\psi(r) = E\psi(r), \tag{2.2}$$

where ψ is the electron envelope function and E is the electron potential energy, in a variational sense [12] with E being a function that takes discrete levels.

From a mathematical point of view, the problem can be seen as an eigenvalue PDE problem. However, it is important to emphasize that both the original model and the derived model (1) have discontinuous coefficients due to different material properties in the QD/WL structure and the barrier. Hence, model (1) should be understood in a generalized sense.

From a physical point of view, one has to view the model (1) as such where the following two conditions should be satisfied (see, e.g. [12])

$$\psi(z, r) \in C(Q), \qquad \frac{-1}{m_e^s \nabla \psi(z, r)} \cdot \boldsymbol{n} = \frac{1}{m_e^b \nabla \psi(z, r)} \cdot \boldsymbol{n}, \qquad (2.3)$$

where $m_e(z, r) = m_e^s$ is the electron effective mass in the QD/WL structure, $m_e(z, r) = m_e^b$ is the electron effective mass in the barrier material, Q is the spatial (r, z) domain of interest, C is the class of continuous functions, and $\boldsymbol{n}$ is outer normal vector in the domain under consideration. Under these circumstances numerical methodologies based on a variational re-formulation of the governing equations is a natural tool in the analysis of these low-dimensional semiconductor structures as soon as realistic geometries and the WL presence are included into consideration. Finally, it should be noted that a special attention should be paid to deriving correct boundary conditions for the entire structure. This issue has been addressed in [10] in detail, and here we use boundary conditions derived from the Ben–Daniel–Duke theory. The problem in hand is reformulated in a variational form, and is discretized by using a finite element approximation.

3. Geometries of coupled QD–WL structures and a three-dimensional model reduction

The importance of the geometry in studying nanostructures has been emphasized in a number of papers (see, e.g. [13]). By now, it is known that the variation in the dot size and shape can produce significant energy fluctuations in the strong confinement region (see, e.g. [7, 11] and references therein). In this paper, we are interested in the analysis of cylindrical, conical, and truncated pyramidal (approximated with truncated conical) QDs which are grown with the Stranski–Krastanov methodology from strained material systems [14]. The dot (that can be grown just a few nanometer in size) and the semiconductor matrix (in which the dot is embedded) are made of lattice-mismatched semiconductors. An important feature of this paper is that the QDs are considered together with the WL. We base our consideration on InAs/GaAs structures, and three basic geometries that are central to our further analysis are presented schematically in figure 1.

In what follows we will analyse numerically how eigenstates, in particular the ground and some of the excited states, in quantum structures are affected by the WL. First, we will follow the line of [10] in finding eigenstates of what we call a 'pure' QD, that is the QD without WL. This means, for example, that in the case of lower plot of figure 1 the layer of thickness 'b' is removed. These results are then compared with the results obtained for the QD with WL. We also analyse in detail the eigenstates of the WL itself. All our structures are cylindrically symmetric. We start our consideration from cylindrical QDs. Then, we use the cone approximation for pyramidal QDs. Finally, the cone approximation of pyramidal QDs is then relaxed to the truncated pyramidal case. For this more realistic approximation, band-structures of three different QDs are reported.

Before proceeding to the actual analysis of the structures specified above, we shall reduce our original three-dimensional model to a simplified one, which can be done if the growth direction is (100) in the geometries represented in figure 1. We shall also describe details of our numerical procedure which is different from the QR algorithm conventionally applied in the context of modelling of low-dimensional structures.
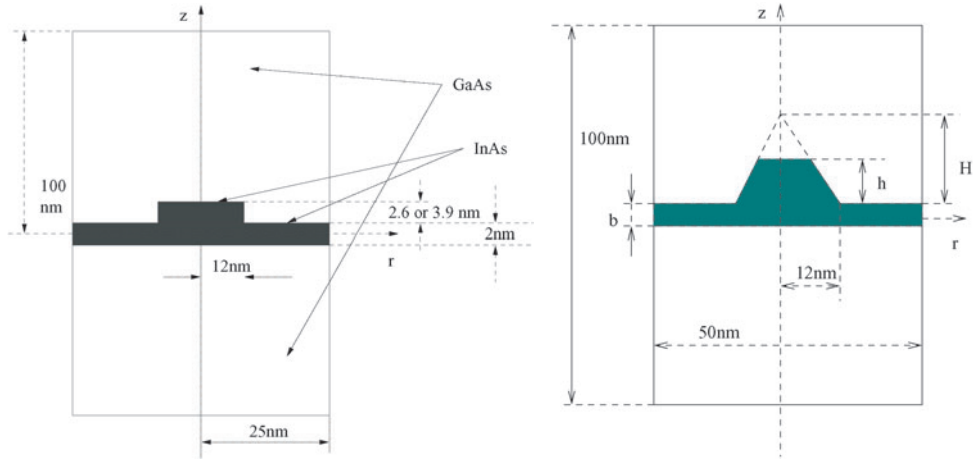
Figure 1. Schematic representation of geometries of quantum dots under consideration: cylindrical (left), conical and truncated pyramidal/conical (right).

First note that for geometries of interest in this paper, the problem cannot be solved analytically. As we have already mentioned, the QD is grown as a few monolayer InAs structure of such shapes as cylindrical, conical or truncated pyramidal. The structure rests on a thin InAs WL, as it is depicted in figure 1. The whole dot/WL InAs structure is embedded in a GaAs crystal matrix. Nevertheless, even for such relatively simple mathematically, but realistic in practice, geometries the resulting model is not amenable to analytical treatments which have been traditionally applied in the physical literature in this context under much simplified assumptions. Note also that taking into account additional effects, such as elastic, thermal, and piezoelectric to name just a few, would necessarily lead to an increasing attention to the development of efficient computational tools for the models discussed in this paper.

The growth direction, considered in this paper as an example, is (100), in which case the model (2.1) and (2.2) allows a separation of variables, and can be reduced to

$$\bar{H}\bar{\psi}(r, z) = E\bar{\psi}(r, z), \qquad \psi(\boldsymbol{r}) = \bar{\psi}(r, z)\bar{\Phi}(\phi), \tag{3.1}$$

where $\bar{\Phi}(\phi)$ is a function of the azimuthal angle only. In this case, by a standard separation-of-variables technique, we can find $\bar{\Phi}(\phi)$ in the explicit form as $\bar{\Phi} = \exp(\mathrm{i}n\phi)$. Here, n (its square, appropriately scaled, gives the constant used for separating variables) is an integer making function $\bar{\Phi}$ a single-valued function such that $\bar{\Phi}(0) = \bar{\Phi}(2\pi)$. Then, the Hamiltonian of the problem under consideration can be represented in the form

$$\bar{H} = -\frac{\hbar^2}{2}\left[\frac{\partial}{\partial r}\left(\frac{1}{m(r, z)}\frac{\partial}{\partial r}\right) + \frac{\partial}{\partial z}\left(\frac{1}{m(r, z)}\frac{\partial}{\partial z}\right)\right] + \frac{\hbar^2 n^2}{2m(r, z)r^2} + V(r, z). \tag{3.2}$$

From a physical point of view, the above model is an approximation obtained within the $\boldsymbol{k} \times \boldsymbol{p}$ framework and we supplemented this model by appropriate boundary conditions which we derived based on the Ben–Daniel–Duke formulations (e.g. [5, 15]), relating the values of the wave function in the dot material and in the crystal matrix. These conditions have been already used in [10]. In (3.2) $m_\mathrm{e}(z, r)$ is the position-dependent electron effective mass and $V_\mathrm{e}(z, r)$ is the position-dependent band-edge potential energy.

4. Numerical procedure: spectral Arnoldi iterations based on Krylov subspaces

Before proceeding to this analysis of band-structures of QDs with WLs, we describe briefly the major advantages of the procedure we use in this paper. In the context of modelling low-dimensional nanostructures, it is the QR algorithm that was granted the most attention (e.g. [5, 16]). However, it should be noted that the standard QR algorithm destroys the sparsity of the matrix, a feature that one does not want to lose in solving large scale eigenvalue problems. For this reason we keep the spectral information about the matrix obtained as a result of our finite element discretization by using what is known as Krylov subspaces [17].

Let us consider this issue in some detail. As we have already mentioned, from a mathematical point of view, model (3.1) and (3.2) supplemented by corresponding boundary conditions is a PDE eigenvalue problem. By using the finite element methodology, the problem is discretized. This leads to a large algebraic eigenvalue problem which should be solved with an efficient iterative procedure. In this paper we solve the corresponding algebraic eigenvalue problem,

$$(A - (E - V)I)\chi_n = f \tag{4.1}$$

with given matrix A and f, with the spectral transformation Arnoldi iterations (see, e.g. [17, 18] and references therein). This Krylov-subspace methodology allows us to deal efficiently with the (large) matrix A resulting from the discretization, by constructing iterations with respect to a sequence of spaces (m is the order of the corresponding Krylov subspace)

$$K_m(A, \chi_n) = \text{span}\{\chi_n, A\chi_n, \ldots, A^{m-1}\chi_n\}. \tag{4.2}$$

To ensure a high accuracy of the results, computations were carried out on a sequence of grids, and all results reported here remain the same after further mesh refinement. The range of computed eigenvalues was specified within the limit given by the barrier energy level. This reduces the computational cost of the problem solution.

5. Computational analysis of electronic states in QD/WL coupled systems

In this section, we present five groups of experiments. First, we consider a cylindrically shaped QD with WL. The size of the dot is 24 nm at the basis (the computational domain is half of this value due to the cylindrical symmetry). The height of the cylinder is 2.6 nm. All other necessary information is provided in figure 1. In all computational experiments reported here we applied the finite element package FEMLAB; we used the conduction-band effective masses $0.023m^*$ and $0.067m^*$ for InAs and GaAs, respectively (m^* is the free electron mass), and band-edge energies -0.697 and 0 for InAs and GaAs, respectively.
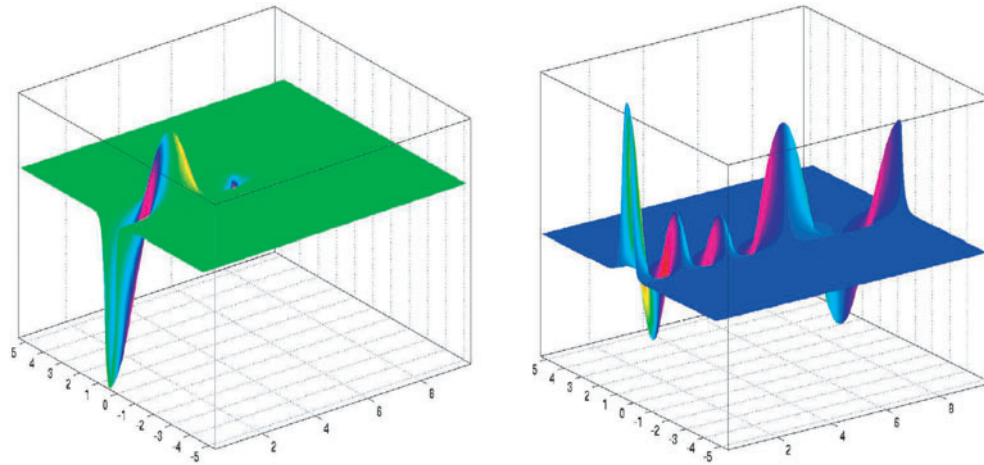
5.1. Cylindrical QDs

In figure 2 we present the ground state and the first three excited states for our cylindrical QD presented in the upper plot of figure 1. The computed eigenvalues are -0.474, -0.324, -0.289, -0.170, respectively (with rounding off all results to include the third digit after the dot only). The mapping of the computational region into the real domain is shown in the caption to figure 2. We follow the same procedure throughout this paper. While the ground state is fully localizable, one can see that the WL influences the electronic states in the dot region. To confirm that, we extended the structure in the r-direction in order to observe whether the wave function would exponentially decay in that case. While for the ground state of this new structure it is indeed the case (see figure 3, left), this cannot be claimed for all excited states (see, e.g. figure 3, right).
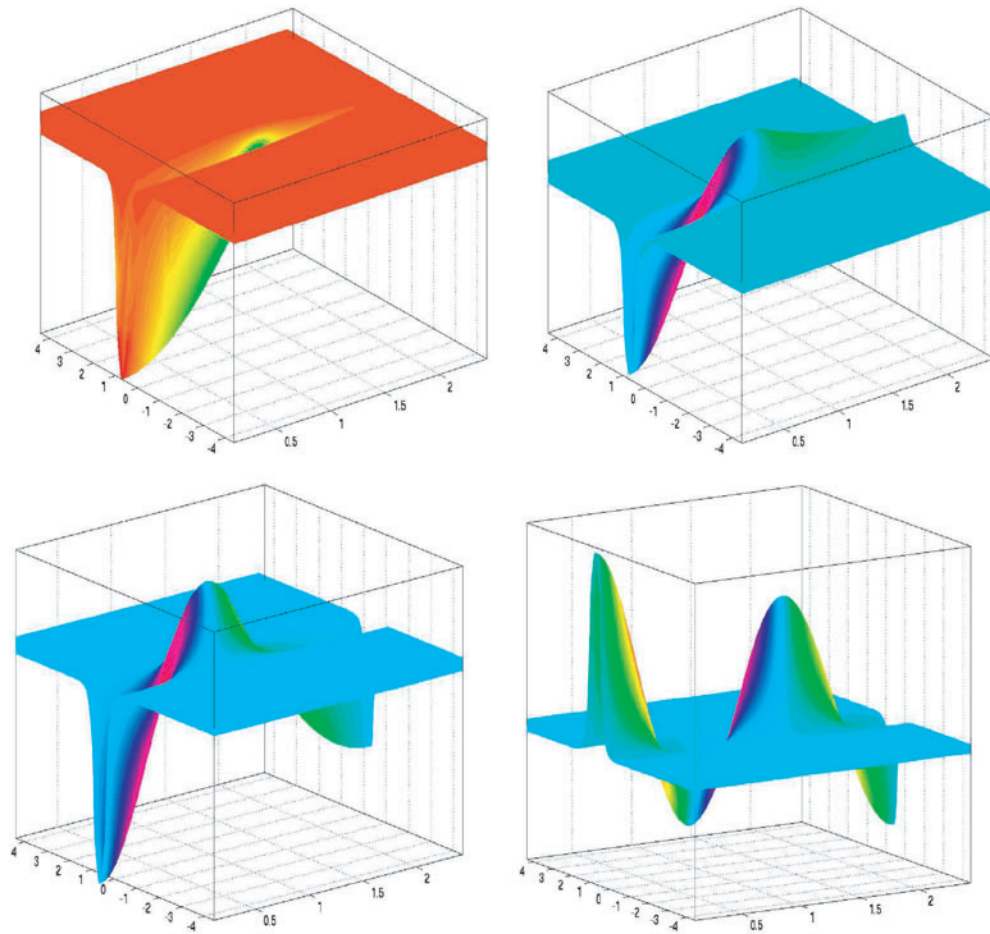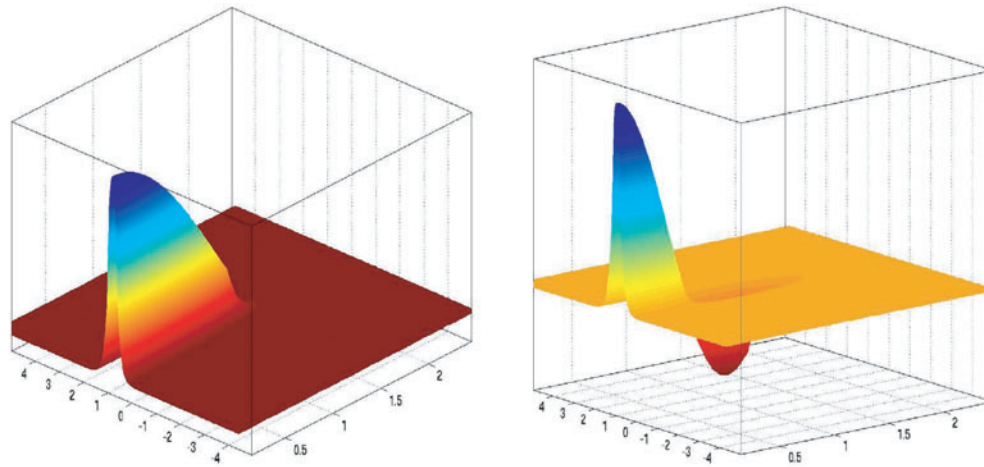
Figure 2. Cylindrical QD with WL: ground state and the first three excited states (the computational domain $(r, z) : 0 \leqslant r \leqslant 2.5, -5 \leqslant z \leqslant 5$ is mapped into the real domain as follows ($r \times 10$ nm, $z \times 10$ nm)).

To make our case stronger, we neglected the WL and considered the 'pure' cylindrical QD. In this case, the ground state (see figure 3, left) is -0.343, which is substantially larger compared to the result obtained for the QD with WL. The first (the only excited state in this case) is -0.186, and this state much better confined compared to the corresponding state in the QD/WL case. The wave functions of these two states are represented in figure 4. As an additional test of our procedure, we also considered the WL only. In this case, the profile of the wave function has a zero-slope shape, as expected, which is typical for quantum wells. This zero-slope shape wave function corresponds to the ground state eigenvalue which has the value of -0.310. The three excited states in this case are -0.281, -0.212, and -0.110.

The next question to answer was whether the coupling phenomena discussed above are an intrinsic feature of cylindrical dots or are they confined to cylindrical QDs of specific size only. By increasing the height of our cylindrical QD by factor of 1.5 and keeping its width the same, for the dot without WL we obtain values of -0.437 and -0.264 for the ground and the first excited state, respectively, which are the only eigenvalues in this case. As expected, these values are smaller compared to the 'pure' QD of smaller height. Finally, we note that

Figure 3. Ground state (left) and the coupled QD/WL excited state corresponding to eigenvalue −0.284 (right) in the extended cylindrical QD.


Figure 4. Cylindrical QD without WL: ground state and the first excited state.

the ground state and the first three excited states for the new QD/WL structure correspond to the values of −0.348, −0.300, −0.182, −0.062, respectively. These values produce wave functions similar to those presented in figure 2, as it is expected, their values are larger compared cylindrical QDs of smaller height with WLs. In figure 5 we present the first (corresponding to the first eigenvalue of −0.348, figure 5, left) and the second excited electronic (corresponding to the third eigenvalue of −0.182, figure 5, right) states of the structure. Similar to the line of reasoning we pursued above, we wanted to make sure that the coupling phenomenon pronounced in figure 5 (right) is generic. For the extended cylindrical structure of this height, we computed electronic states. In figure 6 we present the ground and the second excited states. One can see that while for the ground state the wave function is exponentially decaying in the WL region (figure 6, left), the second excited state clearly demonstrate a strong coupling between electronic states in the entire QD/WL structure. All the above results were obtained for $n = 0$ (see equations (3.1) and (3.2)).
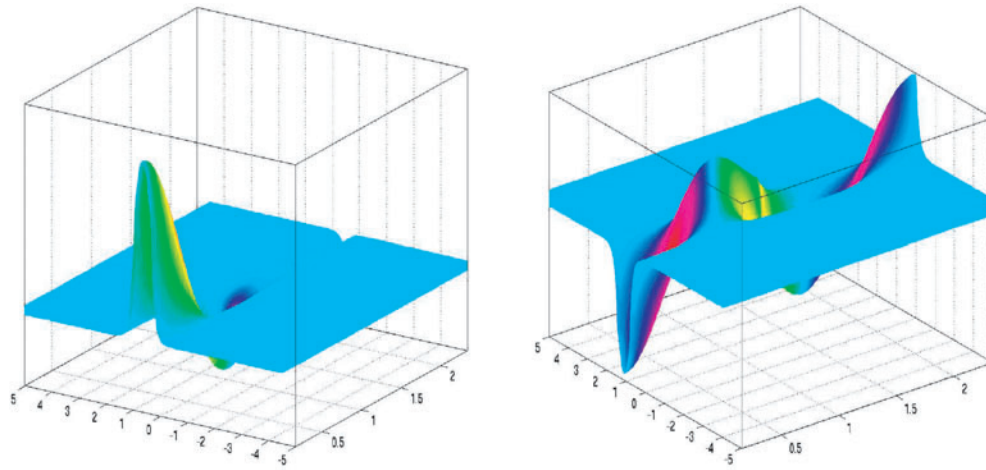
Figure 5. Ground (left) and the second excited states (right) in the QD/WL structure with increased height.
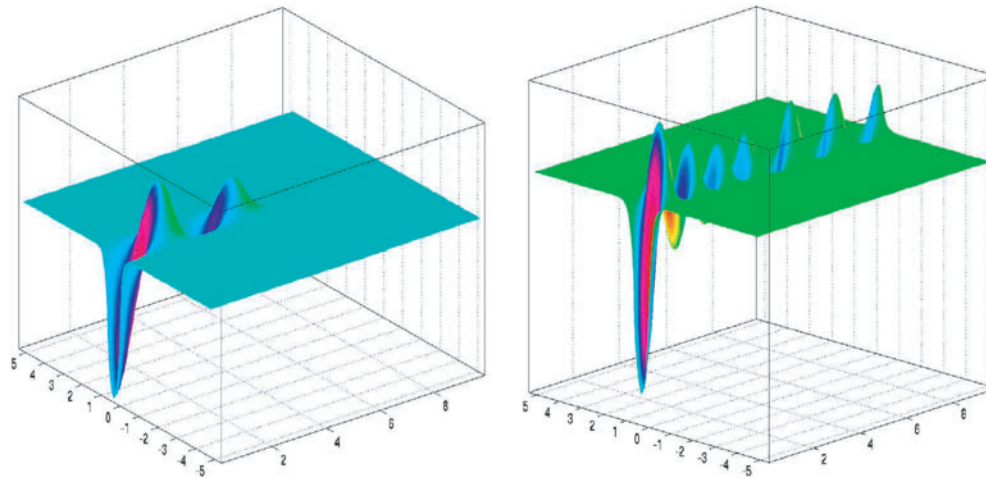

Figure 6. Ground and the second excited states of the extended QD/WL structure with increased height.

5.2. Conical QDs

Our next group of computational experiments follow the line developed originally in [10]. If we consider a conical QD without WL such as that presented in the lower plot of figure 1, we first note that the confinement in this case is well pronounced. Indeed, in figure 7 we present results for $n = 0$ where we observe two states both of which are confined to the dot region. Away from this region the eigenfunctions of these states decrease exponentially quickly in GaAs. Two eigenvalues corresponding to the ground and the first excited states are -0.2482 and -0.0189, respectively. The height of the conical dot in this case is $H = 3$ nm.

However, the situation changes drastically if we include the WL into consideration, that is consider the case which is most realistic in experimentally grown nanostructures. For the WL of thickness $b = 2$ nm (the same as in the case of our cylindrical QD) these changes are
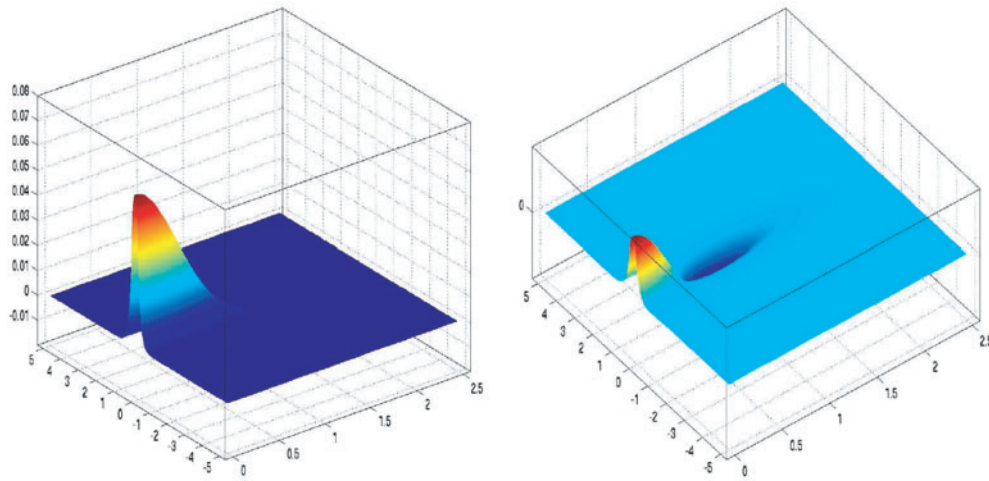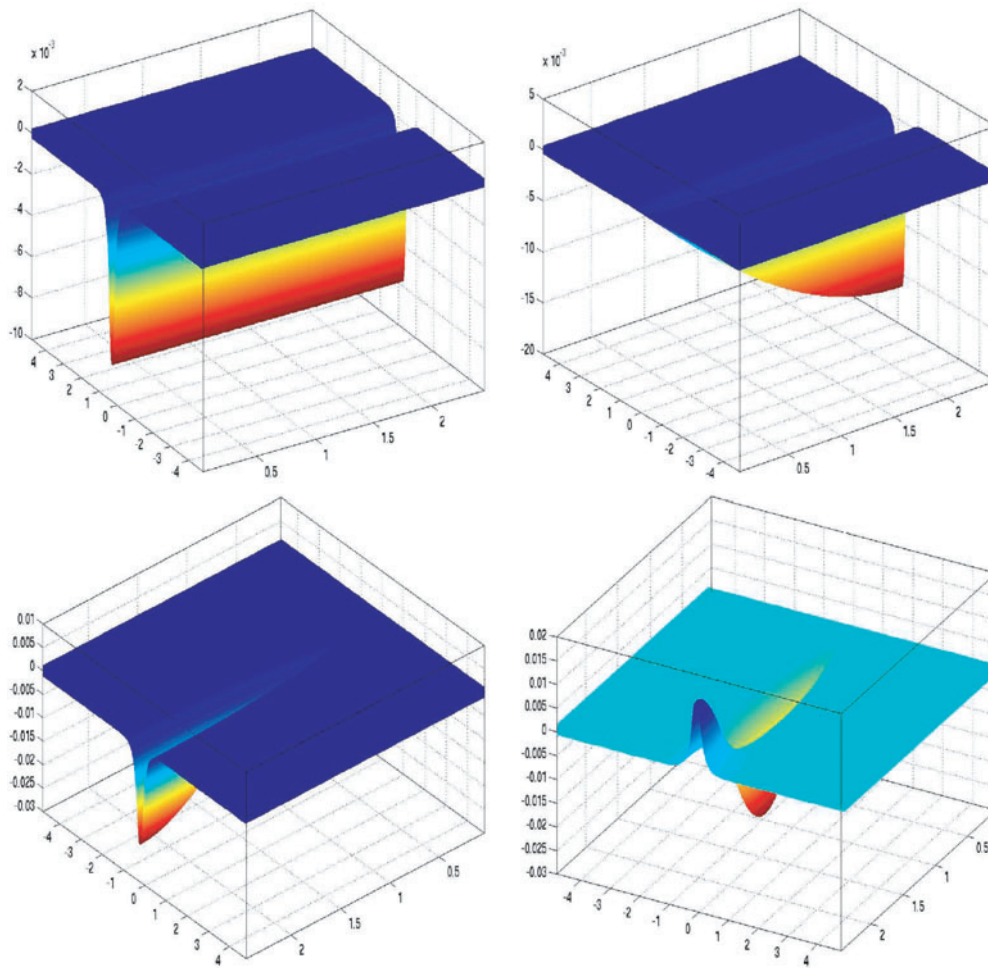
Figure 7. Wave functions of the ground (left) and the first excited (right) states for the conical quantum dot without WL.
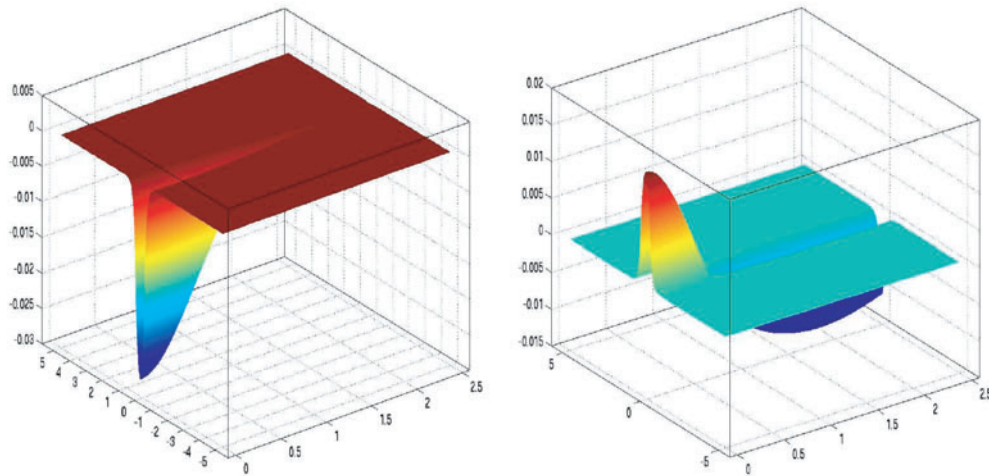
Figure 8. Wave functions of the ground (left) and the first excited (right) states for the conical quantum dot with WL.

twofold. First, the complete structure (QD with WL) has four eigenstates. If we would consider a conical dot of the same height as the height of our cylindrical QD considered before, we would find (see [10]) that the resulting eigenvalues are -0.409, -0.307, -0.253, -0.150, which are higher values compared to their counterparts in the cylindrical case. Second, the actual values of energies for the ground and first excited states are substantially affected by the presence of the WL, which is confirmed by values -0.4203 and -0.3005, respectively for the conical dot of height $H = 3$ nm. Wave functions associated with these states are presented in figure 8. In the terminology of [10], both of the considered above cases are confined to $n = 0$ and $k = 0$. Here, k is a constant entering the envelope function representation in the case where $m(r, z)$ and $V(r, z)$ are piecewise constants (see [15, 10]).

Figure 9. Wave functions of the quantum well WL: ground states for $n = 0, 1$ (upper plots) and the ground and the first excited states for $n = 4$ (lower plots).

The above results show that a more detailed analysis of eigenstates in the WL is required. Apparently the increasing number of states observed in the previous case is due to the presence of the WL. Indeed, four eigenstates are observed for $n = 0, 1$, and 2. With increasing n, the number of eigenstates becomes smaller (three for $n = 2$ and 3; two for $n = 4, 5$, and 6), eventually leading to just one confined state ($n = 7, 8, 9, 10, 11$). We also observe that in terms of the actual values of energies, the ground states of the quantum well WL exhibit a parabolic dependency with increasing values n. Finally, in figure 9 we present wave functions for ground states of the QD WL for $n = 0$ and 1 (left and right upper figures, respectively), and both eigenstates for $n = 4$.

5.3. Truncated pyramidal/conical QD

To analyse the influence of the WL on these structures, we first evaluate eigenstates of truncated conical structures without WL. We observe that the energy of such nanostructures decreases

Table 1. Energy levels of the truncated conical QDs without WL.

Height 2 nm	Height 1.5 nm	Height 1 nm
−0.225 0	−0.1780	−0.1068
−0.010 18	−0.0028	
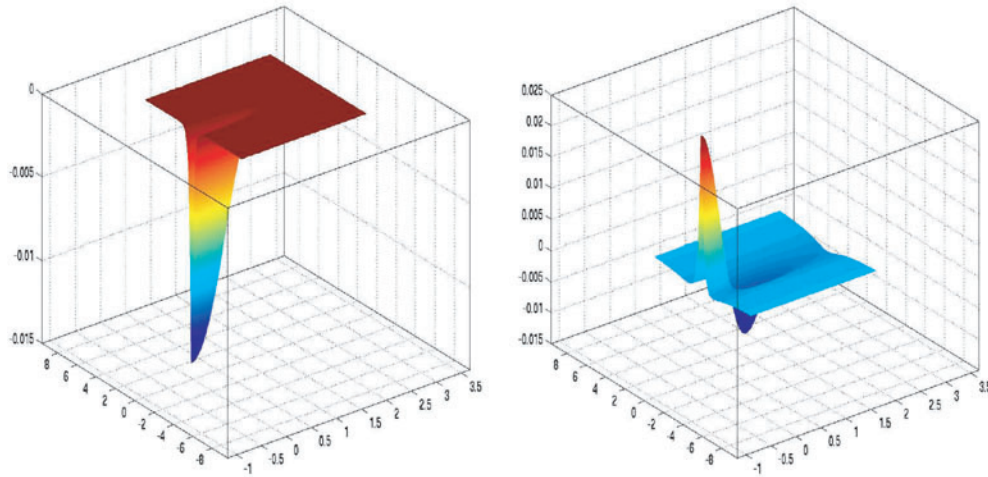
Figure 10. Wave functions of the ground and the first excited states in the truncated pyramidal/conical quantum dot without WL ($h = 1.5$ nm).

**Table 2.** Energy levels of the truncated conical QDs with WL.

Height 2 nm	Height 1.5 nm	Height 1 nm
−0.4142	−0.3998	−0.3755
−0.3057	−0.3047	−0.3032
−0.2516	−0.2462	−0.2396
−0.1491	−0.1451	−0.1404

(in absolute value) with decreasing height (h, see figure 1) of the truncated conical dots. In table 1 we present these observation in a quantitative manner. Note also that for small heights (see, e.g. $h = 1$ nm) only one confined state is observed.

In figure 10 we present wave functions associated with both eigenstates (the ground and the first exited) of the truncated conical QD of height $h = 1.5$ nm. Again, the actual energy values (−0.1780 and −0.0028) are substantially modified if the WL is taken into account.

The number of eigenstates increases to four for all three QD geometries analysed. The actual energy values for truncated QDs with WL are given in table 2, and wave functions associated with the ground and the first excited states of dots with height $h = 1.5$ nm are presented in figure 11.

Finally, in figure 12 we present the results of computations of all four eigenstates for the truncated QD with WL of height 1nm. In this case, only the ground state is a confined dot state, yet even in this case the influence of the WL can be clearly observed. All other states show an intrinsic coupling and state interference.
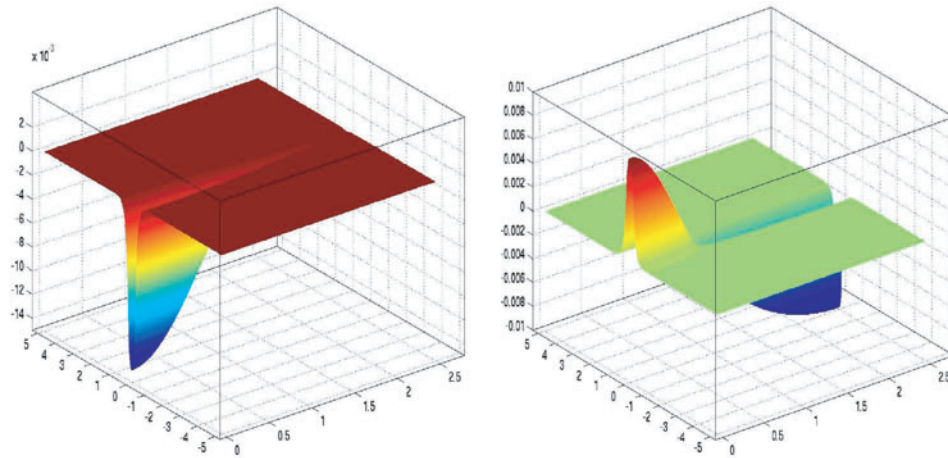
Figure 11. Wave functions of the ground and the first excited states in the truncated pyramidal/conical quantum dot with WL ($h = 1.5$ nm).
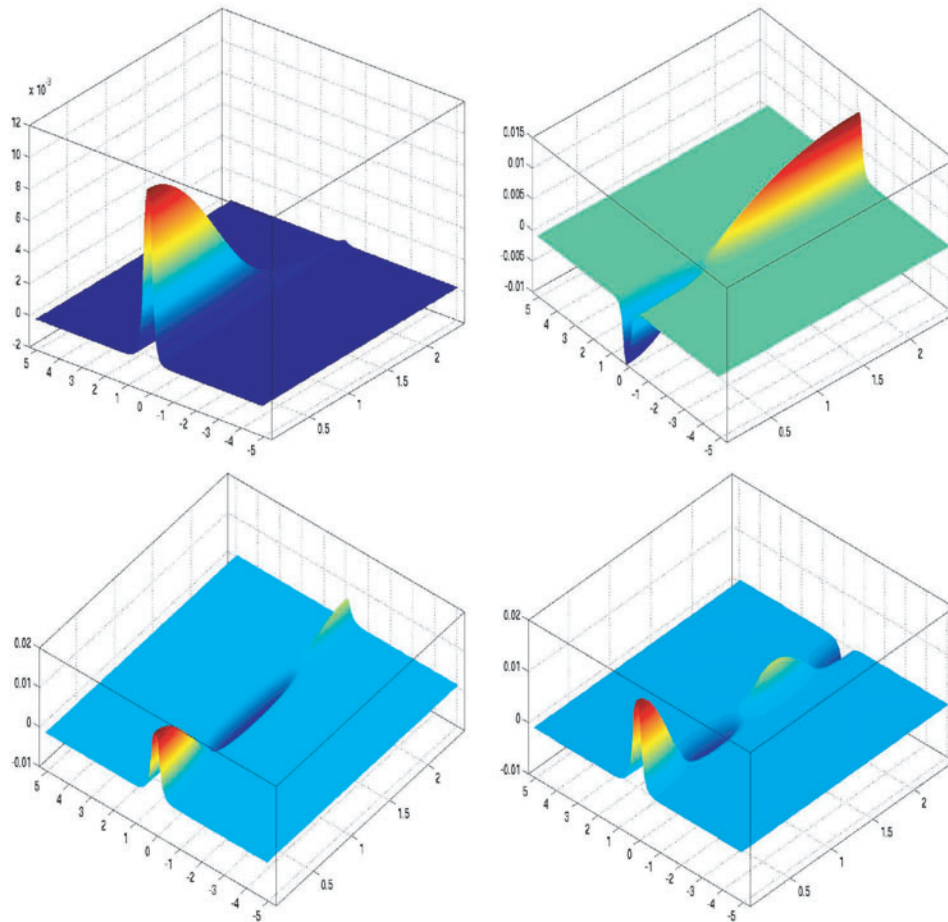
Figure 12. Wave functions of the ground and the first excited states in the truncated pyramidal/conical quantum dot with WL ($h = 1$ nm).

6. Conclusions

In this paper we analysed how the variation in the dot shape may affect energy fluctuations in confinement regions. Our major focus was given to the analysis of cylindrical and truncated conical QDs and their comparisons with earlier obtained results on the fully conical QD nanostructures. The underlying numerical algorithm was based on the Arnoldi iteration technique, which is superior for this class of problems compared to the QR algorithm typically applied in this context. We demonstrated an essential interference between QD and WL states and concluded that in analysing such QD nanostructures coupled electronic states better reflect the physical essence of the problem. For QDs that are intended to be used as active regions in the new generation of electronic and optical devices, the observed effects, originated from the QD–WL coupling, must be taken into account.

Acknowledgment

References

[1] Melnik R V N and He H 2000 Modelling nonlocal processes in semiconductor devices with exponential difference schemes *J. Eng. Math.* **38** 233–63

[2] Williams R L *et al* 2001 Controlling the self-assembly of InAs/InP quantum dots *J. Cryst. Growth* **223** 321–31

[3] Bimberg D, Grundmann M and Ledentsov N N 1998 *Quantum Dot Heterostructures* (UK: Wiley)

[4] Stier O, Grundmann M and Bimberg D 1999 Electronic and optical properties of strained QDs modeled by 8-band $k \cdot p$ theory *Phys. Rev.* B **59** 5688–701

[5] Li Y *et al* 2001 Computer simulation of electron energy levels for different shape InAs/GaAs semiconductor quantum dots *Comput. Phys. Commun.* **141** 66–72

[6] Glas F 2002 Elastic relaxation of isolated and interacting truncated pyramidal quantum dots and quantum wires in a half space *Appl. Surf. Sci.* **188** 9–18

[7] Guffarth F *et al* 2001 Strain engineering of self-organized InAs quantum dots *Phys. Rev.* B **64** art. no. 085305

[8] Werner P *et al* 2000 Quantum dot structures in the InGaAs system investigated by TEM techniques *Cryst. Res. Technol.* **35** 759–68

[9] Adeler F *et al* 1996 Optical transitions and carrier relaxation in self-assembled InAs/GaAs quantum dots *J. Appl. Phys.* **80** 4019–26

[10] Melnik R V N and Willatzen M 2002 Modelling coupled motion of electrons in quantum dots with wetting layers *Proc. Modeling and Simulation of Microsystems (MSM) Conf. (USA, 21–25 April 2002)* pp 506–9 (and *Nanotechnology* 2004 to appear)

[11] Li Y *et al* 2001 Electron energy level calculations for cylindrical narrow gap semiconductor quantum dot *Comput. Phys. Commun.* **140** 399–404

[12] Gelbard F and Malloy K J 2001 Modeling quantum structures with BEM *J. Comput. Phys.* **172** 19–39

[13] Kumagai M and Ohno T 1992 *Solid State Commun.* **83** 837–41

[14] Ledentsov N N 1997 Self-organized quantum wires and dots: new opportunities for device applications *Prog. Cryst. Growth Charact.* **35** 289–305

[15] Bastard G 1988 *Wave Mechanics Applied to Semiconductor Heterostructures* (Halsted Press: New York)

[16] Li Y *et al* 2001 Energy and coordinate dependent effective mass and confined electron states in quantum dots *Solid State Commun.* **120** 79–83

[17] Lehoucq R B 2001 Implicitly restarted Arnoldi methods and subspace iteration *SIAM J. Matrix Anal. Appl.* **23** 551–62

[18] Trellakis A and Ravaioli U 2001 Three-dimensional spectral solution of Schrödinger equation *VLSI Design* **13** 341–7